FJSRL TR-90-0003

FRANK J. SEILER RESEARCH LABORATORY

ALKALI METAL REDUCTIONS AT TUNGSTEN AND MERCURY FILM ELECTRODES IN BUFFERED NEUTRAL ALUMINUM CHLORIDE: 1-METHYL-3-ETHYLIMIDAZOLIUM CHLORIDE MOLTEN SALTS

R.T. Carlin
J. Fulle
J.S. Wilke

AUGUST 1990

AIR FORCE SYSTEMS COMMAND

UNITED STATES AIR FORCE

FJSRL–TR–90–0003

This document was prepared by the Electrochemical Division, Directorate of Chemical Sciences, Frank J. Seiler Research Laboratory, United States Air Force Academy, CO. The reserach was conducted under Project Work Unit number 2303–F2–10, Dr John S. Wilkes was the project officer.

Inquiries concerning the technical content of this document should be addressed to the Frank J. Seiler Research Laboratory (AFSC), FJSRL/NC, USAF Academy, Colorado Springs, CO 80840–6528. Phone AC 719–472–2655.

This report has been reviewed by the Commander and is releasable to the National Technical Information Service (NTIS). At NTIS, it will be available to the general public, including foreign nations.

This technical report has been reviewed and is approved for publication.

JOHN S. WILKES, GM–14
Project Scientist

ALAN A. SHAFFER, Major, USAF
Director, Chemical Sciences

RICHARD J. COOK, Lt Col, USAF
Chief Scientist

Copies of this report should not be returned unless return is required by security considerations, contractural obligations, or notice on a specific document.

Printed in the United States of America. Qualified requestors may obtain additional copies from the Defense Documentation Center. All others should apply to:

National Technical Information Service
6285 Port Royal Road
Springfield VA 22161

REPORT DOCUMENTATION PAGE

Form Approved
OMB No. 0704-0188

1. AGENCY USE ONLY (Leave blank)	2. REPORT DATE	3. REPORT TYPE AND DATES COVERED

4. TITLE AND SUBTITLE Alkali Metal Reductions at Tungsten and Mercury Film Electrodes in Buffered Neutral Aluminum Chloride: 1-Methyl-3-Ethylimidazolium Chloride Molten Salts

5. FUNDING NUMBERS

6. AUTHOR(S)
R.T. Carlin
J. Fuller
J.S. Wilkes

7. PERFORMING ORGANIZATION NAME(S) AND ADDRESS(ES)
FJSRL/NC
USAF Academy
Colorado 80840-6528

8. PERFORMING ORGANIZATION REPORT NUMBER
FJSRL-TR-90-0003

9. SPONSORING/MONITORING AGENCY NAME(S) AND ADDRESS(ES)
AF Office of Scientific Research
Bolling AFB DC 20332

10. SPONSORING/MONITORING AGENCY REPORT NUMBER

11. SUPPLEMENTARY NOTES

12a. DISTRIBUTION/AVAILABILITY STATEMENT
DISTRIBUTION UNLIMITED

Micro Mtr

12b. DISTRIBUTION CODE

13. ABSTRACT *(Maximum 200 words)*
Alkali metal reductions from MCl (M= Li, Na, and K) buffered neutral $AlCl_3$: ImCl melts at a bare 250-μm diameter tungsten electrode and at the same tungsten electrode coated with a mercury film were studied. In the LiCl buffered neutral melt, bulk Li deposition occurs before the cathode limit of the melt; however, the deposited Li reacts then rapidly with the imidazolium cation. Sodium and potassium are not deposited at the bare tungsten electrode in melts buffered with the appropriate alkali metal chloride. At the mercury film electrode (MFE), deposition and stripping of Li, Na, and K were observed at -1.18, -1.35, and -1.68 V in buffered neutral melts. By comparison to aqueous reduction potentials, the formal potentials for deposition of the pure alkali metals from buffered neutral melts are predicted from the experimentally determined formal potentials of the alkali metal amalgams in the melts. (TTL)

14. SUBJECT TERMS	15. NUMBER OF PAGES
	35
	16. PRICE CODE

17. SECURITY CLASSIFICATION OF REPORT	18. SECURITY CLASSIFICATION OF THIS PAGE	19. SECURITY CLASSIFICATION OF ABSTRACT	20. LIMITATION OF ABSTRACT
UNCLASSIFIED	UNCLASSIFIED	UNCLASSIFIED	UNLIMITED

INTRODUCTION

The ambient-temperature chloroaluminate molten salt $AlCl_3$:1-ethyl-3-methylimidazolium chloride (ImCl) has proven to be a useful solvent for investigating the electrochemistry of organic and inorganic materials (1,2). In melts with an $AlCl_3$:ImCl molar ratio > 1 (N > 0.5, where N is the $AlCl_3$ mole fraction), termed acidic melts, the anodic limit is determined by the oxidation of the $AlCl_4^-$ anion, and the cathodic limit is set by reduction of the $Al_2Cl_7^-$ anion to Al metal. In melts with an $AlCl_3$:ImCl molar ratio < 1 (N < 0.5), termed basic melts, the anodic limit is determined by chloride oxidation, and the cathodic limit is set by reduction of the imidazolium cation. Finally, at an $AlCl_3$:ImCl ratio = 1 (N = 0.5), a neutral melt, the anodic and cathodic limits are determined by $AlCl_4^-$ oxidation and imidazolium reduction, respectively, providing a wide electrochemical window of ca. 4.4 V (3). Although desirable, this wide electrochemical window is difficult to achieve and maintain since electrochemical processes can alter the composition of the melt by producing or consuming the electroactive components of the melts. Examples of electrochemical processes which alter the composition of the melt are shown in reactions [1] and[2].

$$M \text{ (electroactive metal)} + 2n\, AlCl_4^- \text{ <===> } MCl_n^{(n-x)-} + n\, Al_2Cl_7^- + x\, e^- \quad [1]$$

$$Cl_2 + 2\, e^- \text{ <===> } 2\, Cl^- \quad [2]$$

Recently, it has been reported that NaCl added to an initially acidic melt (excess $AlCl_3$) can be employed as a "buffer" to maintain the neutral composition (4). The alkali metal chloride neutralizes the $Al_2Cl_7^-$ species via reaction [3];

$$NaCl(s) + Al_2Cl_7^- \text{ <===> } Na^+ + 2\, AlCl_4^- \quad [3]$$

yet the solubility of the alkali metal chloride in the buffered neutral melt is negligible preventing introduction of excess choride ions. Therefore, when $Al_2Cl_7^-$ or chloride ions are introduced into the buffered neutral melt, they are removed via reactions [3] and [4], respectively.

$$Na^+ + Cl^- \text{ <===> } NaCl(s) \quad [4]$$

Because Na^+ is not normally reduced before the imidazolium cation, the wide electrochemical window is maintained (4). Similar buffering is achieved for LiCl; however, Li^+ is reduced before

the imidazolium cation, thus, narrowing the electrochemical window (5). Incomplete buffering is achieved for KCl and CsCl, i.e., the solubilities of these alkali metal salts in the acidic melts appear to be too low to completely neutralize the melt by reaction [3].

Of primary interest to the work performed at the Frank J. Seiler Research Laboratory is the development of high energy density batteries based on these ambient-temperature molten salts, including the alkali metal buffered melts. Recently, an evaluation of various battery configurations employing these molten salts has been published as a Technical Report by R. L. Vaughn (6). The evaluation is comprehensive, describing earlier as well as the most recent developments in this area, and should be consulted to fully appreciate the chemical reactions occurring at the anodes and cathodes proposed for these molten salt batteries. Batteries employing a NaCl buffered melt as the electrolyte with solid Na as the anode and CuCl (secondary battery) or $CuCl_2$ (primary battery) as the cathode demonstrate promising characteristics; however,the performance of the battery is hampered by reaction of the solid Na with the melt forming a passivating layer on the Na surface. Similar reactions have been noted for solid Li in the melts (5,7). In addition, Li metal reacts with ImCl in acetonitrile (8) in a similar manner as the reaction of N-alkyl-imidazoles with Li metal and Li reagents (9).

To provide further insight into the chemistry of the alkali metals in these melts, we initiated an examination of the electrochemistry of the alkali metals at a 125-μm radius tungsten disk electrode. The small size of the electrode makes possible electrochemical studies of electroactive species present in high concentrations (10). In addition, it is relatively easy to fully coat such a small electrode with mercury, thus producing a mercury film electrode (MFE) at which deposition of alkali metals occurs at a much less negative potential due to formation of alkali metal amalgams. From the reduction potentials for these amalgams it is possible to predict the reduction potentials for the alkali metals themselves.

To our knowledge the only other study of metal deposition at a mercury electrode in an ambient-temperature melt is that for Al in acidic $AlCl_3$:ImCl (11). Also, relevant to this work is a study of the electrical double layer at a hanging mercury drop electrode in the $AlCl_3$:1-butylpyridinium chloride ambient-temperature molten salt (12).

EXPERIMENTAL

ImCl was synthesized as previously described except diethyl ether was used in place of ethyl acetate for the recrystallization (2). All melt preparations and electrochemical experiments were performed under a purified He atmosphere in a Vacuum Atmosphere dry box at 27 °C. Melts were prepared by addition of sublimed $AlCl_3$ (Fluka) to ImCl with stirring until the desired molar ratio was obtained. For preparation of an alkali metal chloride buffered melt, an acidic melt with an $Al_2Cl_7^-$ concentration equal to the desired alkali metal ion concentration was first prepared. A quantity of the alkali metal chloride in excess of that needed to neutralize the $Al_2Cl_7^-$ (reaction [3]) was then added, and the mixture was stirred overnight at room temperature. The concentration of the alkali metal in the resulting neutral buffered melt was taken to be the initial $Al_2Cl_7^-$ concentration, i.e., no correction was made for the change in the density of the melt. This correction is expected to be < 5 % since this is the maximum density change observed for the same $AlCl_3$:ImCl acidic melts neutralized with ImCl (13).

The tungsten working electrode consisted of a length of 250-μm diameter tungsten wire (Alpha Chemical) sealed in 1-mm I.D. Pyrex glass capillary tubing. The end of the glass was ground to expose a circular disk of tungsten which was polished with alumina powder.. The reference electrode consisted of an Al wire immersed in an acidic 1.5:1.0 $AlCl_3$:ImCl melt (N = 0.6) contained in a separate glass capillary tube in which a fiberglass fiber was sealed at one end to make electrical contact with the analyte solution. The counter electrode consisted of an Al wire dipped directly into the analyte solution. The cell consisted of a glass vessel fitted with a Teflon cap through which three holes were drilled to allow insertion of the electrodes into the melts.

Cyclic staircase voltammetry and chronoamperometric experiments were performed using an EG&G PARC Model 273 Potentiostat/Galvanostat controlled with the EG&G PARC 270 software package.

RESULTS AND DISCUSSION

Lithium Deposition at a Bare Tungsten Electrode

In a LiCl buffered melt ([Li] = 0.564 M, starting with N = 0.53) bulk deposition of Li was observed at ca. -1.9 V on the bare 250-μm diameter tungsten electrode while Li stripping was negligible, Figure 1. The apparent small stripping current may not be Li anodization, but instead, may be associate with the passivating film which is deposited on the tungsten electrode following the Li deposition. To obtain reproducible results, it was necessary to wipe the electrode between each electrochemical experiment to remove this film. The film is probably a product of the reaction of Li with the imidazolium cation (8,9). It is doubtful that the lack of sufficient Li stripping is due to protonic impurities because of the large quantity of Li^+ reduced. The behavior of Li is in agreement with a previous study (5).

The results of staircase cyclic voltammetric experiments are summarized in Table I. The peak potential shifts to more negative potentials with increasing scan rate, v, while the value of $I_p/v^{1/2}$ remains relatively constant. These trends are consistent with a reversible electron transfer followed by an irreversible chemical process, i.e., an E_rC_i mechanism (14). The peak potential shift is larger than expected (theoretical: 30/n mV negative shift for a ten-fold increase in v), but the additional potential shift may be due in part to IR-drop. If the Li deposition is actually an E_rC_i process, then E_p will actually be positive of the formal potential (14). Additional, features can be seen in Figure 1 at potentials positive of that for bulk Li deposition. Of particular note is the small cathodic spike at ca. -1.2 V which has been associated with underpotential deposition of Li (7).

By starting with an acidic melt and titrating the $Al_2Cl_7^-$ with LiCl, it is possible to observe both Al and Li deposition. By adding 0.103 g LiCl to 14 g of a 0.53 $AlCl_3$:ImCl melt ($[Li^+]$ = 0.28 M and $[Al_2Cl_7^-]$ = 0.33 M) the voltammogram shown in Figure 2 is obtained. The Al deposition and stripping waves are obvious at potentials slightly negative of 0 V, and Li^+ reduction is seen at ca. -1.9 V. Continued addition of LiCl eventually produces a buffered neutral melt, and Li^+ reduction is the only major electrochemical process observed. It is noteworthy that for melts

partially neutralized with LiCl, small cathodic and anodic features are again observed in the voltammograms at potentials between the aluminum and lithium electrochemistry. These features may be associated with Li underpotential deposition, as well as an interaction between Al and Li; however, there is no justification for invoking the formation of a LiAl alloy at this time. Underpotential deposition and stripping of Li is clearly observed in Figure 3 for a partially neutralized melt. Finally, it appears that Al deposition may occur in melts presumed to be fully buffered, as shown in Figure 4, where the cathodic wave at -0.9 V is believed to be due to Al deposition.

To better quantitate the Li^+ reduction process, chronoamperometric experiments were performed at potentials from -1.7 to -2.2 V. It was again necessary to wipe a film from the electrode following each chronoamperometric experiment. The Li^+ reduction, Figure 5, shows the classic features - rapid rise followed by a $t^{-1/2}$ decay - for a deposition process involving nucleation followed by diffusion controlled growth of the nuclei (15).

Employing chronoamperograms recorded at potentials from -1.7 to -2.2 V, voltammograms equivalent to normal pulse voltammograms can be constructed. It is not possible to perform ordinary normal pulse experiments because of electrode fouling following each pulse. Voltammograms constructed from a series of chronoamperograms recorded in a 0.55 melt are shown in Figure 6. Because of the complications resulting from the nucleation phenomenon, the shape of the waves require a more detailed analysis than can be performed at this time. However, a diffusion-limited current plateau is clearly achieved for all times at potentials negative of -2.05 V.

Several buffered neutral melts with different concentrations of Li^+ were made, and chronoamperograms were recorded for several potentials on the diffusion-limited current plateaus. The chronoamperograms were plotted as I vs. $1/t^{1/2}$, and straight lines were visually fitted to these plots using an option in the computer software. Generally, behavior approaching linearity was observed for times from 100 ms to 1 s. From the slopes of these lines, values for the diffusion coefficient for Li^+ were calculated employing the Cottrell equation (14). Results are summarized in Table II. The Li^+ diffusion coefficient does not show a consistent trend as a function of melt composition; however, this is likely a result of the influence of the nucleation phenomenon and the

electrode fouling. The overall average diffusion coefficient, 3.2 x 10^{-7} cm^2 s^{-1}, is considerably lower than the value of (8.6 ± 0.3) x 10^{-7} cm^2 s^{-1} for Li^+ diffusion determined using a tungsten rotating disk electrode in neutral melts containing low Li^+ concentrations (< 200 mM) (5). This may be due to the higher viscosities of buffered neutral melts containing alkali metal chlorides compared to neutral melts containing only low concentrations of the alkali metal chlorides (16).

Alkali Metal Deposition at a Mercury Film Electrode (MFE)

To lower the reduction potential for alkali metal deposition, a mercury film was deposited on the 250-μm diameter tungsten electrode. The deposition was performed in a $AlCl_3$:ImCl acidic melt (N = 0.60) containing 50 mM $HgCl_2$. The staircase cyclic voltammogram for mercury in Figure 7 shows good deposition and stripping behavior and agrees with a previous study (17). The mercury film electrode (MFE) was prepared by holding the potential at -0.6 V for 400 s with stirring. It was necessary to immediately remove the electrode from the deposition solution because the Hg deposit is unstable toward reaction with Hg^{2+} to form Hg^+. The mercury deposit appears to be stable in the buffered neutral melt.

Figures 8, 9, 10 show voltammograms for Li, Na, and K deposition and stripping, respectively, at the MFE from buffered neutral melts made by saturating $AlCl_3$:ImCl acidic melts (N = 0.53) with the appropriate alkali metal halide. The alkali metal amalgams appear to be stable in the melts. Figure 11 shows clearly the negative shift in the reduction potentials in going from Li to K.

The reduction potentials for the alkali metal amalgams are shifted positive from the reduction potential of the pure alkali metal by an amount corresponding approximately to the free energy of formation of the alkali metal amalgam, reaction 5.

$$xM(s) + yHg \text{ <===> } M_xHg_y \qquad [5]$$

At the MFE, the reduction occurs as in reaction [6], and the reduction potential is less negative than the reduction potential at a bare electrode, reaction [7].

$$M^+ + e^- + Hg \text{ <===> } M(Hg) \qquad [6]$$

$$M^+ + e^- \text{ <===> } M \qquad [7]$$

The full equation describing the shift in potential is found in the polarographic literature (18) and is

given by

$$E_a^o = E_M^o + E_s + (0.0591/n)\log C_{satd.} f_{satd.} - (RT/nF)\ln(a_{Hg}^*) \quad [8]$$

where E_a^o is the standard potential for the amalgam, E_M^o is the standard potential of the pure metal, E_s is equal to $-\Delta G/nF$ (ΔG = free energy change for reaction [5]), $C_{satd.}$ and $f_{satd.}$ are the solubility and activity coefficient, respectively, of the metal in mercury, and a_{Hg}^* is the activity of mercury in the saturated amalgam. All the terms in Eq. [8] except E_a^o and E_M^o should be the same in aqueous and molten salt solvents because there is no reason to expect the alkali metal amalgams to differ in the two media. Therefore, from examination of reduction potentials in aqueous systems, it is possible to estimate the formal potential for the alkali metals in the buffered neutral melt. The results are summarized in Table III. It is important to point out that the alkali metal formal potentials at mercury are basically "eyeballed" from the cyclic voltammograms and so, have errors of at least ± 50 mV. However, from the data in Table III, it is possible to see that only Li and Na hold promise as battery anodes in the buffered neutral $AlCl_3$:ImCl melts; the reduction potential for K is too negative. Both Li and Na have calculated reduction potentials very near the cathode end of the electrochemical window. This is consistent with the bulk reduction of Li^+ discussed above. Also, with a properly handled tungsten electrode, it is possible to observe Na deposition and stripping at a potential negative of -2 V; the tungsten electrode, in this case, shows a very high overpotential for Im^+ reduction (19).

Despite the ability to observe the deposition of pure Li^+ (and pure Na^+ under special circumstances), the deposited Li does not appear to be stable in the melt. It is important to note that the reduction of Im^+ is shifted +250 mV at a platinum electrode versus tungsten (20). The platinum catalyzes the Im^+ reduction, while tungsten has a higher overpotential for Im^+ reduction allowing observation of Li^+ reduction. Therefore, Li metal is actually thermodynamically unstable in the buffered neutral melt with a possible reaction path being that in reaction [9] (9). If Li^+ is formed in the reaction, then it will precipitate as LiCl and will passivate the Li metal surface.

Reaction [9]

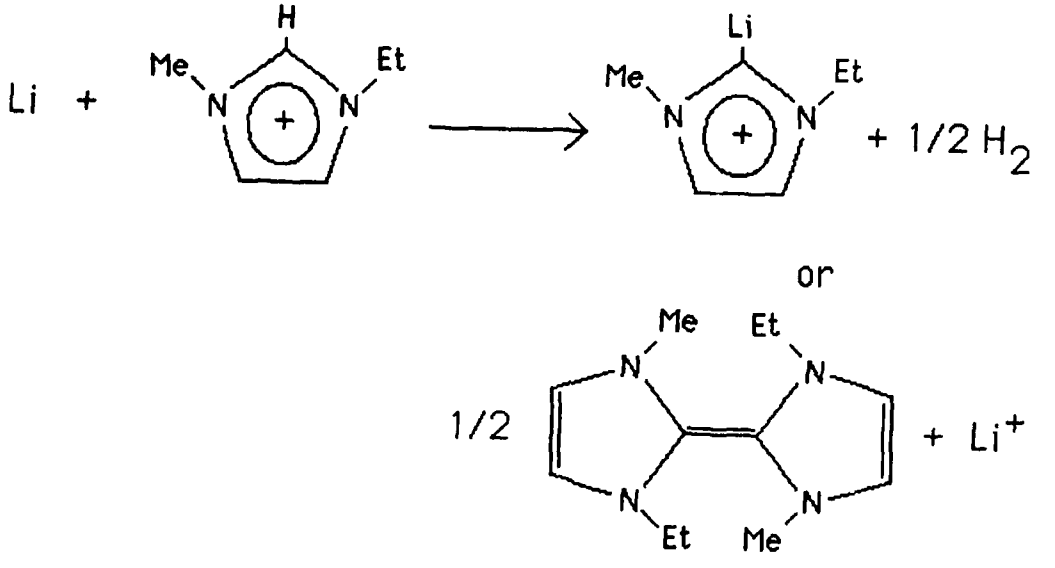

The deposition and stripping waves in Figures 8 - 11 are rather broad and show features suggestive of more than one electrochemical process occurring. This is probably a result of saturation of the mercury film caused by the high concentration of the alkali metals being reduced. For Li, Na and K, it is possible to form several amalgam phases richer in the alkali metal than that formed in the dilute regime (21). These alkali metal- rich phases will have a different free energy of formation and, therefore, a different reduction potential. This is nicely demonstrated in Figure 12 in which a slower scan rate was employed for Na^+ reduction allowing a larger quantity of Na to deposit and strip; two distinct electrochemical processes are observed.

Proton Removal with Sodium Metal

Since the presence of NaCl in the melt is not deleterious to its performance, it is possible to use Na metal to remove protons from the melt. Sodium metal added to an acidic melt reacts with protonic impurities, reaction [10], and produces an active Al, reaction [11], which also reacts with protons.

$$Na + H^+ \text{------>} Na^+ + H_2 \qquad [10]$$

$$3\,Na + 4\,Al_2Cl_7^- \text{-----> } 3Na^+ + Al + 7\,AlCl_4^- \qquad [11]$$

This offers a simple method for removing protonic impurities from acidic melts.

SUGGESTIONS FOR FUTURE WORK

1. Bulk Li deposition in the $AlCl_3$:ImCl should be better quantitated, and the chemical reactivity of Li with Im^+ further examined. The use of an inverted microscope for viewing the deposition process would be invaluable.

2. Other chloroaluminate molten salts employing C-2 derivatized imidazolium (20) and quaternary ammonium (22, 23) cations should be examined for alkali metal deposition. The small extension of the cathodic end of the electrochemical window for chloroaluminate melts based on these organic cations may prevent reaction of Li and Na with the melts. Also, blocking the C-2 position on the imidazolium cation should stabilize it towards reaction with the alkali metals.

3. The deposition of the alkali metals, as well as other active metals, e.g. Mg, should be better studied at mercury film electrodes (MFE) or at a hanging mercury drop electrode (HMDE). This data can be used to predict the stability of the metals in the melt. Improvements in the properties of the MFE can be achieved employing iridium based microelectrodes (23). Again, an inverted microscope for viewing the MFE would be most useful.

4. The behavior of LiAl alloys, as well as other alloys (Li_5Si, LiAlMg, etc), should be examined. The potential of the LiAl alloys with 10 - 46% Li will be ca. 400 mV positive of Li metal at room temperature. This positive shift in the potential may be enough to prevent reaction with Im^+.

REFERENCES

1. C. L. Hussey, in "Advances in Molten Salt Chemistry," Vol. 5, G. Mamantov, Editor, p. 185, Elsevier, Amsterdam (1983).

2. J.S. Wilkes, J. A. Levisky, R. A. Wilson, and C. L. Hussey, Inorg. Chem., **21**, 1263 (1982).

3. M. Lipsztajn and R. A. Osteryoung, J. Electrochem. Soc., **130**, 1968 (1983).

4. T. J. Melton, J. Joyce, J. T. Maloy, J. A. Boon, and J. S. Wilkes J. Electrochem. Soc., in press.

5. M. Lipsztajn and R. A. Osteryoung, Inorg. Chem., **24**, 716 (1985).

6. R. Larry Vaughn, "Evaluation of Room-Temperature Chloroaluminate Molten Salts as Electrolytes for High Energy Density Batteries," FJSRL-TR-90-0001, Frank J. Seiler Research Laboratory, USAF Academy, April 1990.

7. B. J. Piersma and J. S. Wilkes, 1990 SFRP Report.

8. Lithium metal reacts vigorously with ImCl in acetonitrile liberating hydrogen. The ^{1}H NMR indicates loss of the proton at the C-2 position. R.T. Carlin, T. A. Zawodzinski, Jr. and R. A. Osteryoung, unpublished results.

9. M. R. Grimmett, in "Comprehensive Heterocyclic Chemistry," Vol. 5, Part 4A, A. R. Katritsky and C. W. Rees, Editors, p. 415, Pergamon Press, New York (1984).

10. R. T. Carlin and R. A. Osteryoung, J. Electroanal. Chem., **252**, 81 (1988).

11. R. Moy and F. M. Donahue, Electrochimica Acta, **33**, 721 (1988).

12. R. J. Gale and R. A. Osteryoung, Electrochimica Acta, **25**, 1527 (1980)

13. A. A. Fannin, D. A. Floreani, L. A. King, J. S. Sanders, B. J. Piersma, D. J. Stech, R. L. Vaughn, J. S. Wilkes, and J. L. Williams, J. Phys. Chem., **88**, 2614 (1984).

14. A. J. Bard and L. R. Faulkner, "Electrochemical Methods," Wiley, New York (1980).

15. R. Greef, R. Peat, L. M. Peter, D. Pletcher, and J. Robbinson, "Instrumental Methods in Electrochemistry," T. J. Kemp, Editor, Ellis Horwood Ltd., Chichester, England (1985).

16. A. Elias and J. S. Wilkes, unpublished results.

17. Bernard J. Piersma and John S. Wilkes, "Electrochemical Surv f Selected Cations and Electrode Materials in Dialkylimidazolium Chloroaluminate Melts," FJSRL-TR-82-0004, Frank J. Seiler Research Laboratory, USAF Academy, September 1982.

18. I. M. Koltoff and J. J. Lingane, "Polarography," Vol.1, 2nd Edition, (1952).

19. J. A. Boon and J. S. Wilkes, unpublished results.

20. P. R. Gifford and J. B. Palmisano, J. Electrochem. Soc., **134**, 610 (1987).

21. M. Hansen, "Constituion of Binary Alloys," 2nd Edition, McGraw-Hill, New York (1958).

22. S. D. Jones and G. E. Blomgren, J. Electrochem. Soc., **136**, 424 (1989).

23. J. R. Stuff, S. W. Lander, Jr., J. W. Rovang, and J. S. Wilkes, J. Electrochem. Soc., **137**, 1492 (1990).

24. C. Wechter and J. G. Osteryoung, Anal. Chem., 2092 (1989)

25. N. P. Yao, L. A. Heredy, and R. C. Saunders, J. Electrochem. Soc., **118**, 1039 (1971).

Table I. Staircase Cyclic Voltammetric Data for Lithium Reduction ($[Li^+]$ = 0.56 M) at a 250-μm Tungsten Electrode from a LiCl Buffered Neutral $AlCl_3$:ImCl Melt.

Scan Rate, v ($V\ s^{-1}$)	E_p, (V)	I_p, (μA)	$I_p/v^{1/2}$, ($\mu A\ V^{-1/2}\ s^{1/2}$)
0.500	-2.03	33.6	47.5
0.200	-1.94	20.2	45.1
0.100	-1.92	16.1	50.9
0.050	-1.91	11.2	50.1

Table II. Data for Chronoamperograms Recorded for Lithium Reduction at a 250-μm Tungsten Electrode from LiCl Buffered Neutral $AlCl_3$:ImCl Melts.

N	$[Li^+]$ (M)	E (V)	Cottrell Slope (μA $s^{1/2}$)	Intercept (μA)	D (cm^2 s^{-1})[a]
0.58	1.54	-2.15	24.2	19.8	
		-2.10	26.7	11.1	3.5×10^{-7}
		-2.05	24.1	6.19	
0.56	1.14	-2.15	18.0	9.74	
		-2.10	16.2	10.8	2.90×10^{-7}
		-2.05	16.6	8.45	
0.54	0.729	-2.15	11.4	3.93	
		-2.10	11.2	5.73	3.37×10^{-7}
		-2.05	11.9	3.72	
0.52	0.380	-2.15	5.18	1.36	
		-2.10	5.18	1.06	2.62×10^{-7}
		-2.05	5.24	1.12	
				Overall Average D:	3.2×10^{-7}

[a]Average diffusion coefficient for the melt.

Table III. Formal Potentials for Alkali Metal Reduction in Water and Buffered Neutral $AlCl_3$:ImCl Melts.

	$E^{o'}$, Aqueous Solution (vs. H^+/H_2)		$E^{o'}$, Buffered Neutral Melt (vs. Al/Al^{3+})	
	$M^+/M(Hg)$[a]	M^+/M[b]	$M^+/M(Hg)$[c]	M^+/M[d]
Li	-2.10	-3.045	-1.18	-2.12
Na	-1.863	-2.711	-1.35	-2.20
K	-1.887	-2.924	-1.68	-2.71

[a] Measured in 0.1 M Me_4NCl; 0.1 M Me_4NOH, J. Heyrovsky and J. Kuta, "Principles of Polarography," Academic Press, New York (1966).

[b] CRC, 62nd Edition.

[c] Estimated from staircase cyclic voltammograms in Figures 8 - 10.

[d] Calculated using:

$$E^{o'}, M^+/M(melt) = E^{o'}, M^+/M(Hg)(melt) + [E^{o'}, M^+/M(aq) - E^{o'}, M^+/M(Hg)(aq)]$$

PN Model 270 Electrochemical Analysis Software FV 1.00
EXT CV EXPERT CYCLIC VOLTAMMETRY DR 07-18-90 TR 09:14:07
NORMAL PT PASS CP 0.000 vs. OC CT PASS DT PASS IP 0.560 vs. R ET 5
VI -2.200 vs. R VD PASS V2 0.000 vs. OC FP 0.500 vs. R SI 0.005 SR 2.201E-01 ST 2.499E-02
NC 1 SC 1 AM RAMP CR 10 UA NP 1001 RU 0.000E+00 IR NONE
PL NONE RT HIGH STABILITY
——— lia136.dat

Figure 1. Staircase cyclic voltammogram ($\nu = 200$ mV s^{-1}) for reduction of Li^+ at a 250-μm diameter tungsten electrode in a $AlCl_3$:ImCl melt (N = 0.53) buffered with LiCl ([Li^+] = 0.56 M).

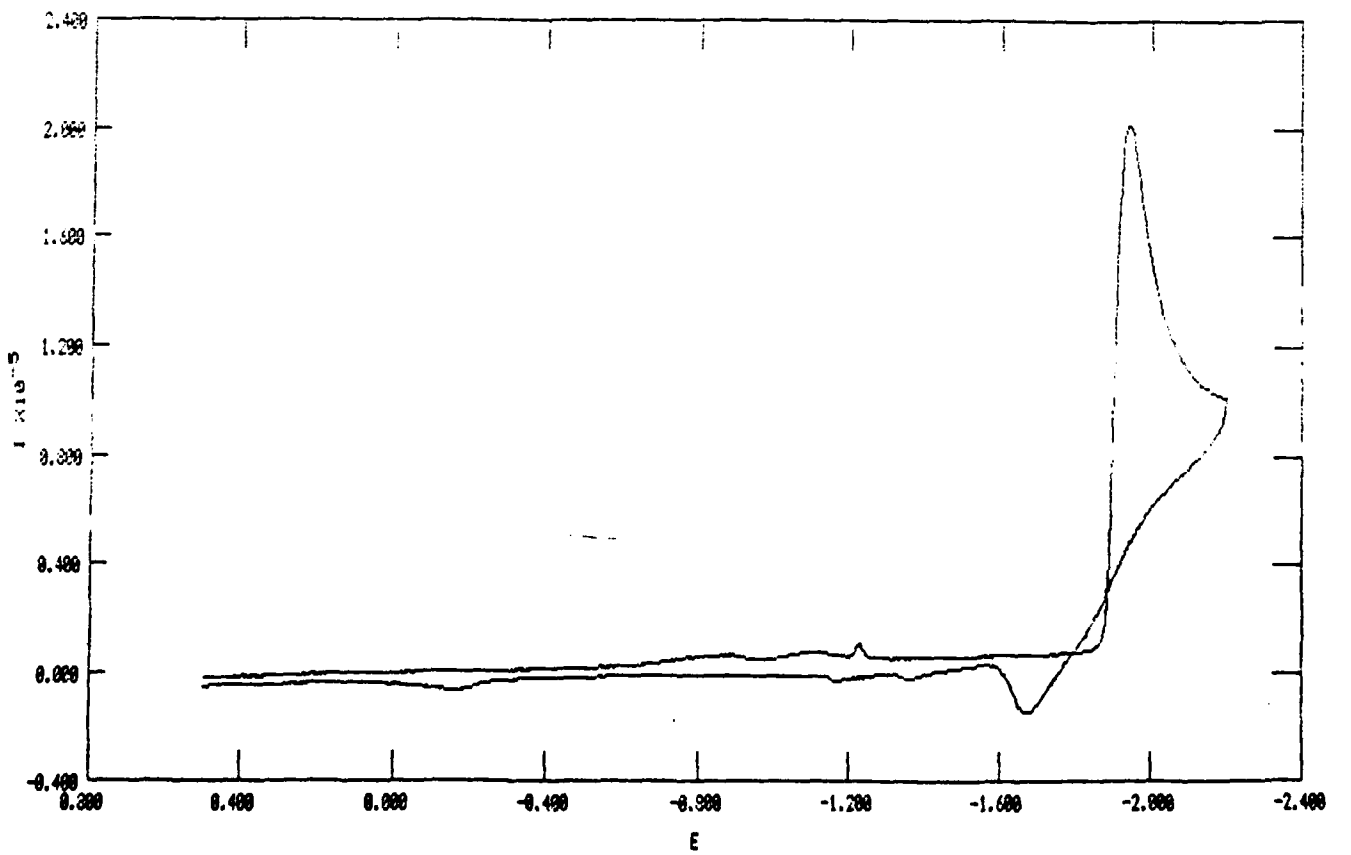

PN Model 270 Electrochemical Analysis Software FV 1.00
EXT CV EXPERT CYCLIC VOLTAMMETRY DR 07-17-90 TR 12:39:18
NORMAL PT PASS CP 0.000 vs. OC CT PASS DT PASS IP 0.500 vs. R ET 5
VI -2.200 vs. R VD PASS V2 0.000 vs. OC FP 0.500 vs. R SI 0.305 SR 1.000E-01 ST 4.995E-02
NC 1 SC 1 AM RAMP CR 100 UA NP 1001 RU 0.000E+00 IR NONE
FL NONE RT HIGH STABILITY
lial12.dat

Figure 2. Staircase cyclic voltammogram ($v = 100$ mV s^{-1}) for reduction of $Al_2Cl_7^-$ and Li^+ at a 250-μm diameter tungsten electrode in a $AlCl_3$:ImCl melt (N = 0.53) partially neutralized with LiCl ($[Li^+] = 0.23$ M and $[Al_2Cl_7^-] = 0.33$ M).

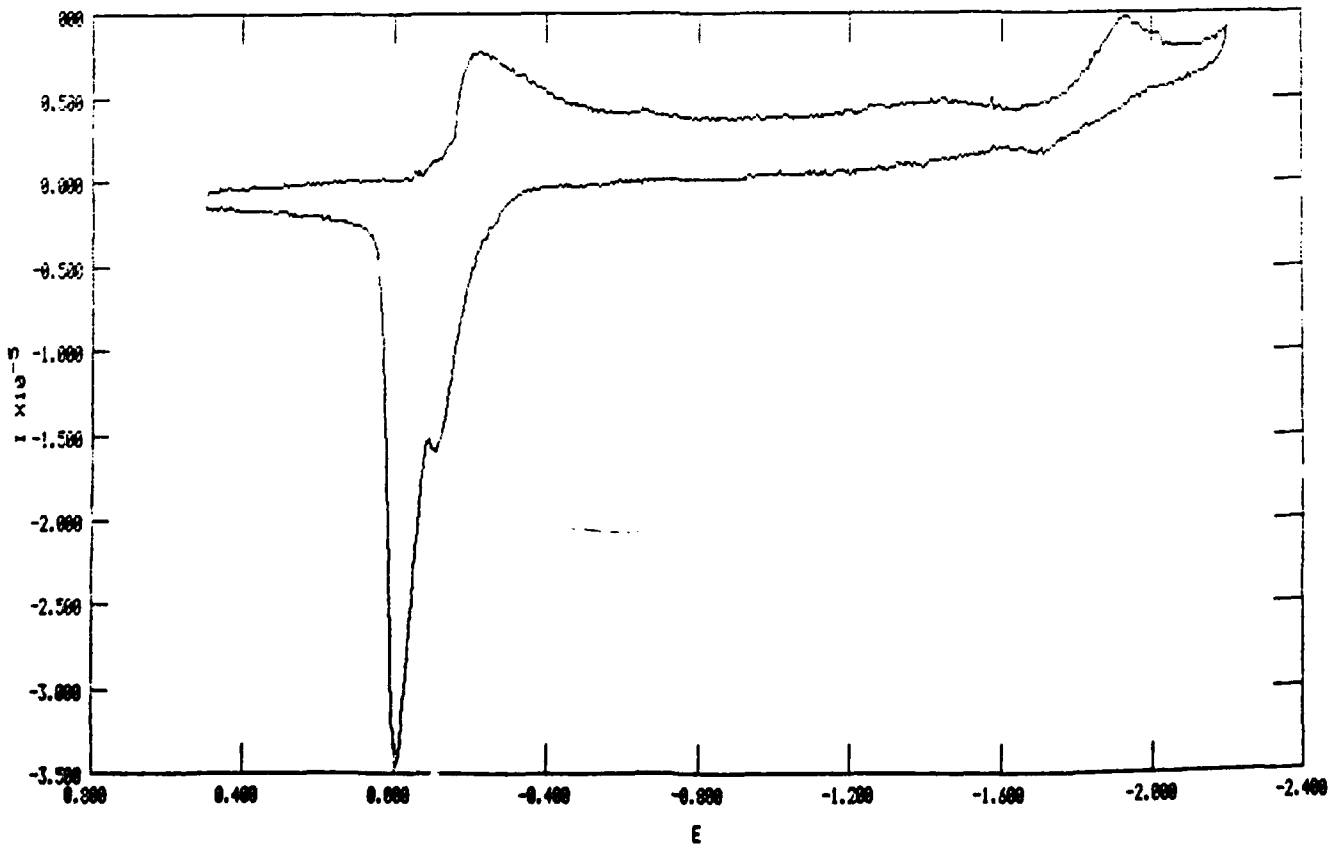

```
PN  Model 270 Electrochemical Analysis Software          FV  1.00
EXT CV  EXPERT CYCLIC VOLTAMMETRY      DR  07-17-90     TR  11:12:32
NORMAL          PT  PASS               CP    0.000 vs. OC CT  PASS          DT  PASS          IP    0.500 vs. R  ET  5
V1   -1.800 vs. R  VD  PASS            V2    0.000 vs. OC FP    0.500 vs. R SI    0.005       SR  5.000E-01    ST   1.200E-02
SC  1              SC  1               AM  RAMP           CR  100 UA        NP  921           RU  0.000E+00    IR  NONE
FL  NONE           RT  HIGH STABILITY
_____  lia15.dat
```

Figure 3. Same melt and electrode as Figure 2, but $\nu = 500$ mV s^{-1}, and the potential is reversed at -1.8 V.

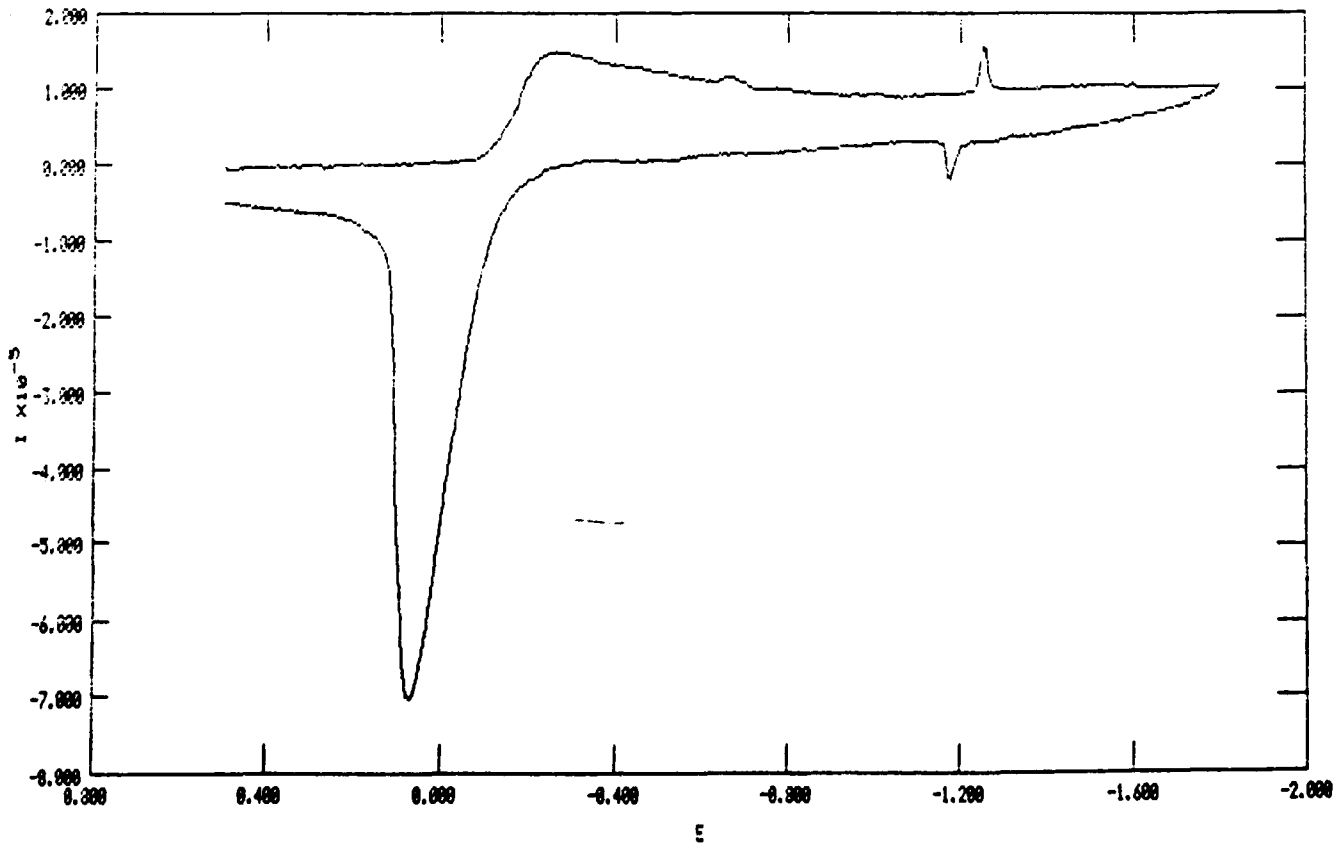

```
PN  Model 270 Electrochemical Analysis Software          FV  1.00
EXT CV  EXPERT CYCLIC VOLTAMMETRY       DR  07-27-90     TR  15:22:54
NORMAL              PT  PASS            CP   0.200 vs. OC  CT  PASS              DT  PASS        IP   0.200 vs. R   ET  2
VI  -2.200 vs. R    VD  PASS            V2   0.000 vs. OC  FP   0.200 vs. R      SI   0.002      SR. 5.000E-01     ST  4.000E-03
NC  1               SC  1               AM  3AMP           CR  100 UA            NP  2401        RU  0.000E+00     IR  NONE
FL  NONE            RT  HIGH STABILITY
______  cv53.dat
```

Figure 4. Staircase cyclic voltammogram ($\nu = 500$ mV s^{-1}) for reduction of Li^+ at a 250-μm diameter *tungsten* electrode in a $AlCl_3$:ImCl melt (N = 0.55) buffered with LiCl ($[Li^+] = 0.94$ M).

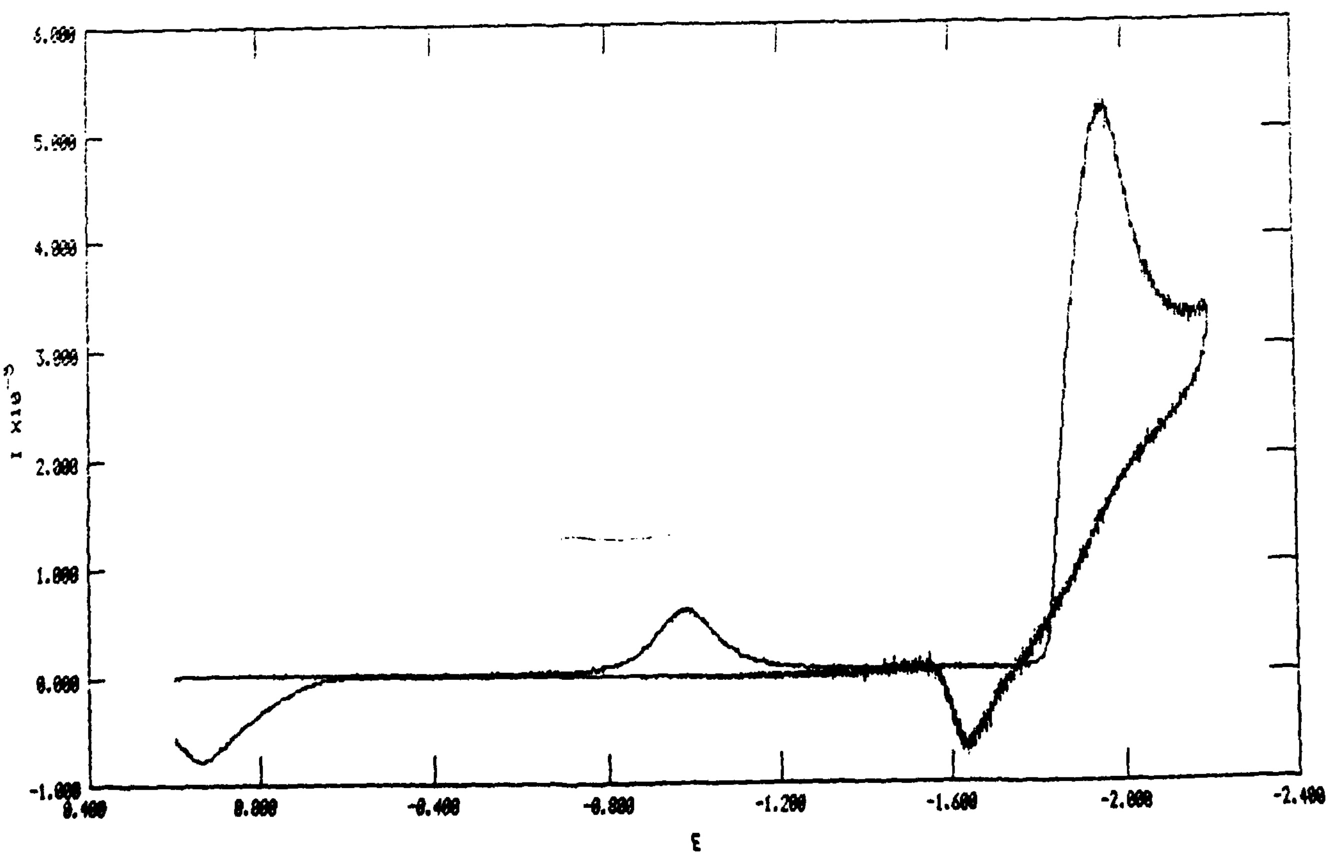

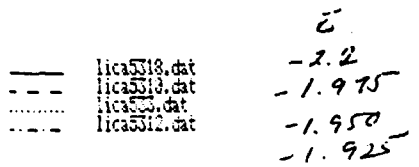

Figure 5. Chronoamperograms for reduction of Li^+ at a 250-μm diameter tungsten electrode in a $AlCl_3$:ImCl melt (N = 0.55) buffered with LiCl ([Li^+] = 0.94 M). Reduction potentials: (a) -2.2 V, (b) -1.975 V, (c) -1.95 V, (d) -1.925 V.

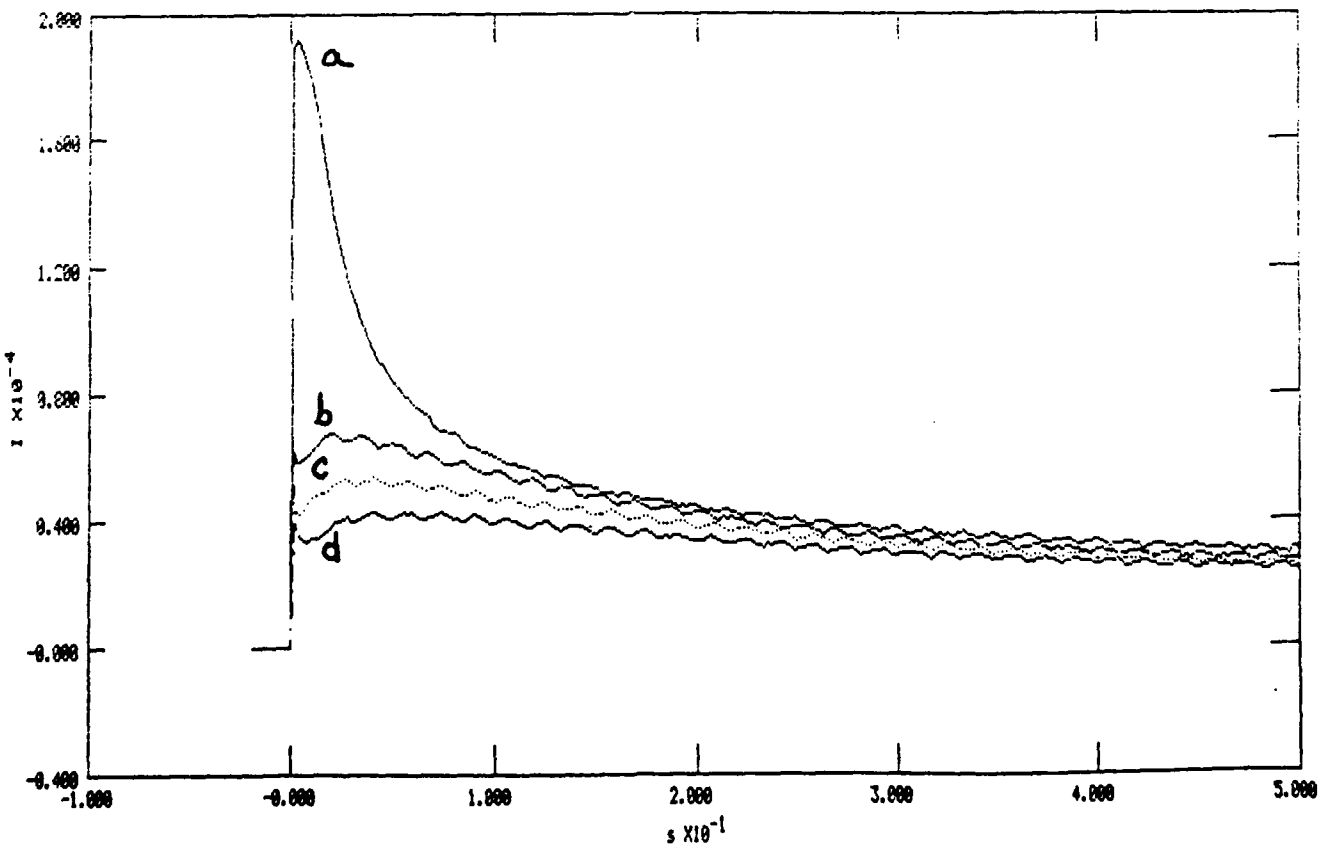

Figure 6. Voltammograms constructed from a series of chronoamperograms recorded for reduction of Li^+ at a 250-μm diameter tungsten electrode in a $AlCl_3$:ImCl melt (N = 0.55) buffered with LiCl ([Li^+] = 0.94 M). Times: (a) 60 ms, (b) 100 ms, (c) 189 ms, (d) 589 ms, (e) 1120 ms.

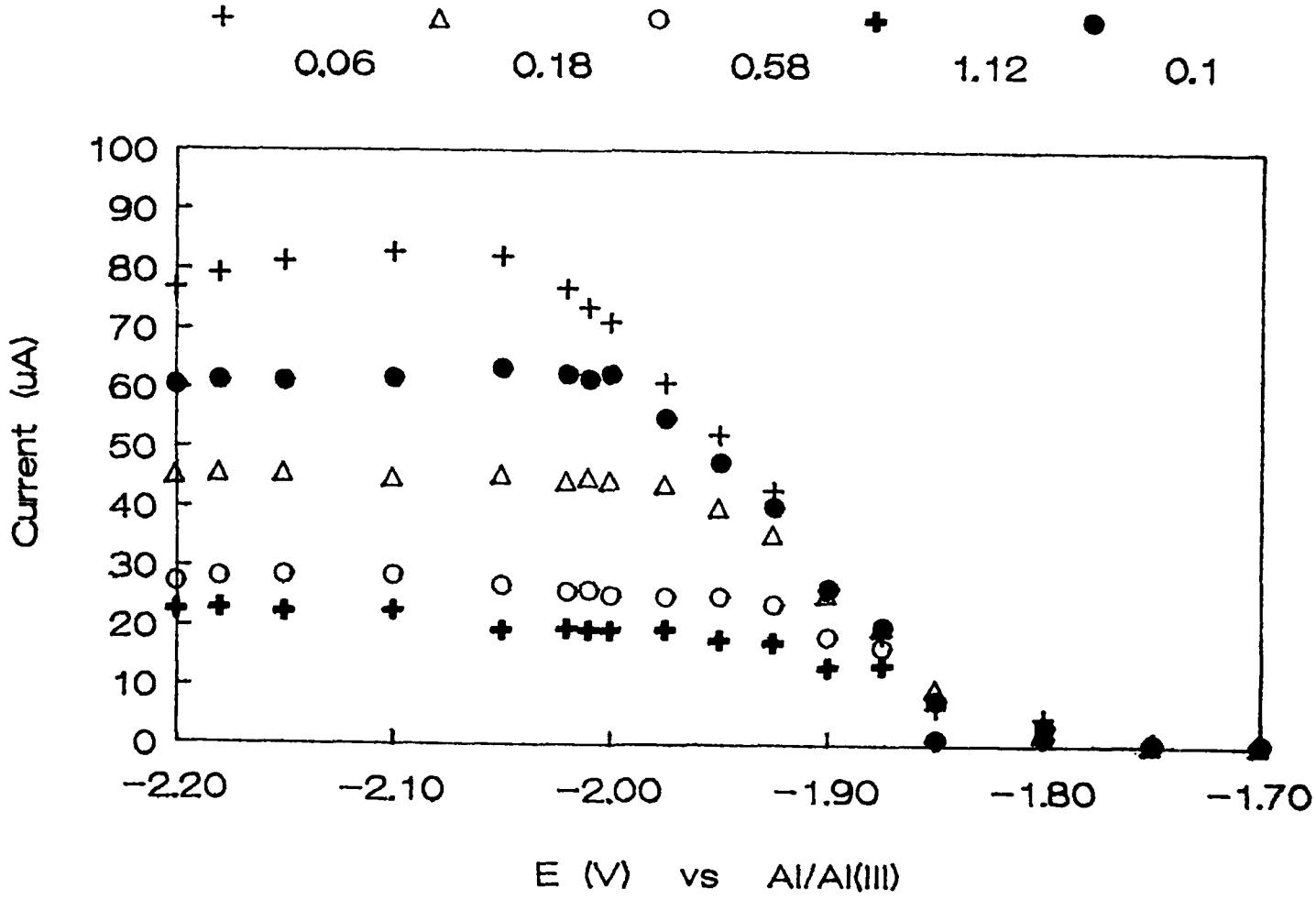

```
EN  Model 270 Electrochemical Analysis Software          FV   1.00
EXT DV  EXPERT CYCLIC VOLTAMMETRY       DR  07-16-98     TM  15:37:29
NORMAL          PT  PASS                CP    0.000 vs. OC  CT  PASS          DT  PASS        IP    1.500 vs. R  ET  5
VI    0.200 vs. R   VB  PASS            V2    0.000 vs. OC  FP    1.500 vs. R  SI    0.005     SR   1.000E-01    ST   4.999E-02
NC  1               SC  1               AM  RAMP          CR  100 UA          NP  521         RU  0.000E+00     IR  NONE
FL  NONE            RT  HIGH STABILITY
      hg=3.dat
```

Figure 7. Staircase cyclic voltammogram (ν = 100 mV s^{-1}) for reduction of Hg^{2+} at a 250-μm diameter tungsten electrode in a $AlCl_3$:ImCl melt (N = 0.60) containing 50 mM $HgCl_2$.

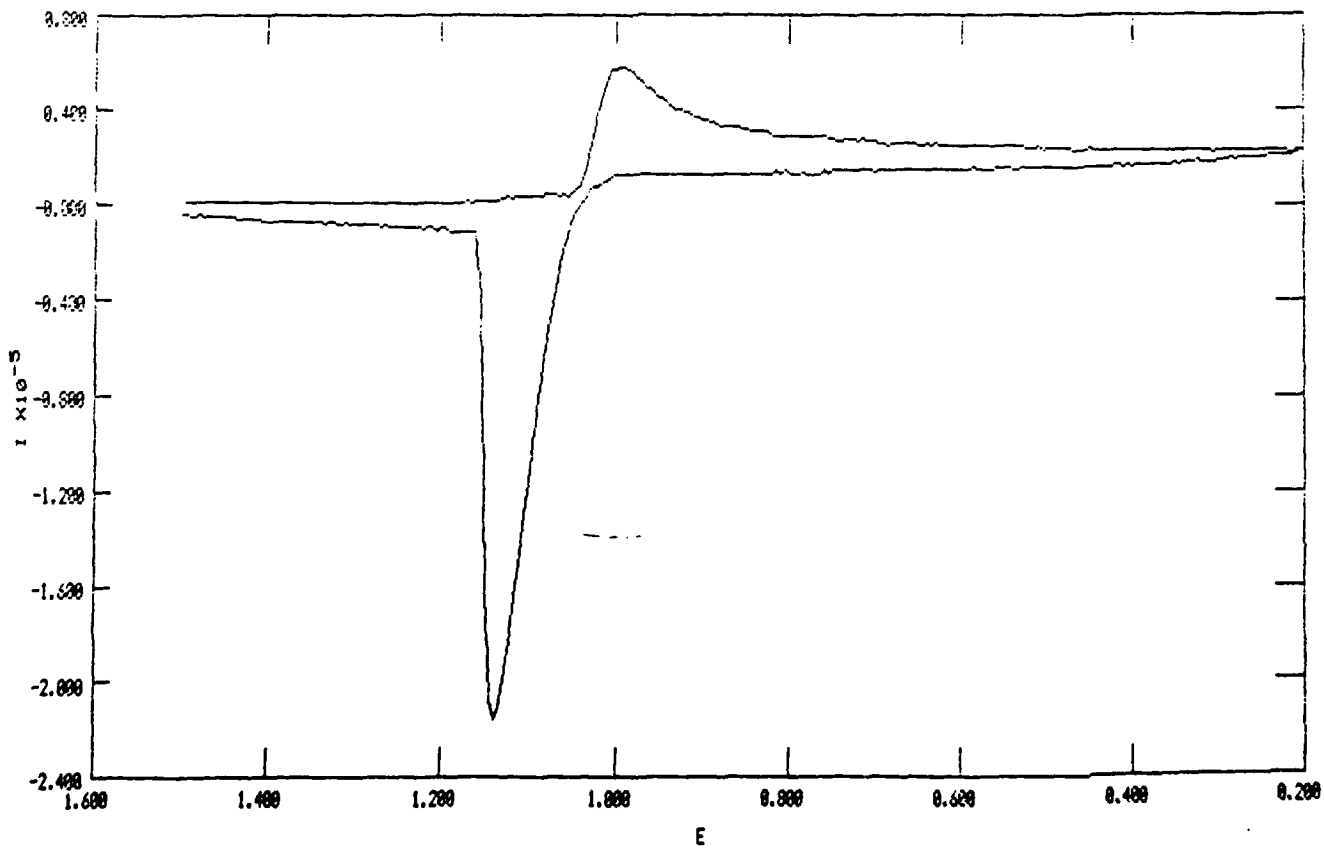

PN Model 270 Electrochemical Analysis Software FV 1.00
EXT CV EXPERT CYCLIC VOLTAMMETRY DR 07-30-90 TR 13:48:47
NORMAL PT PASS CP 0.000 vs. OC CT PASS DT PASS IP -0.600 vs. R ET 2
VT -1.500 vs. R VD PASS V2 0.000 vs. OC FP -0.500 vs. R SI 0.002 SR [illegible] ST 4.000E-02
NC 1 SC 1 AH RAMP CR 100 uA NP 1001 RU 0.000E+00 IR NONE
FL NONE ST HIGH STABILITY
hg113.dat

Figure 8. Staircase cyclic voltammogram (ν = 500 mV s^{-1}) for deposition and stripping of Li at a mercury film deposited on a 250-μm diameter tungsten electrode. Melt is $AlCl_3$:ImCl (N = 0.53) buffered with LiCl ([Li^+] = 0.56 M).

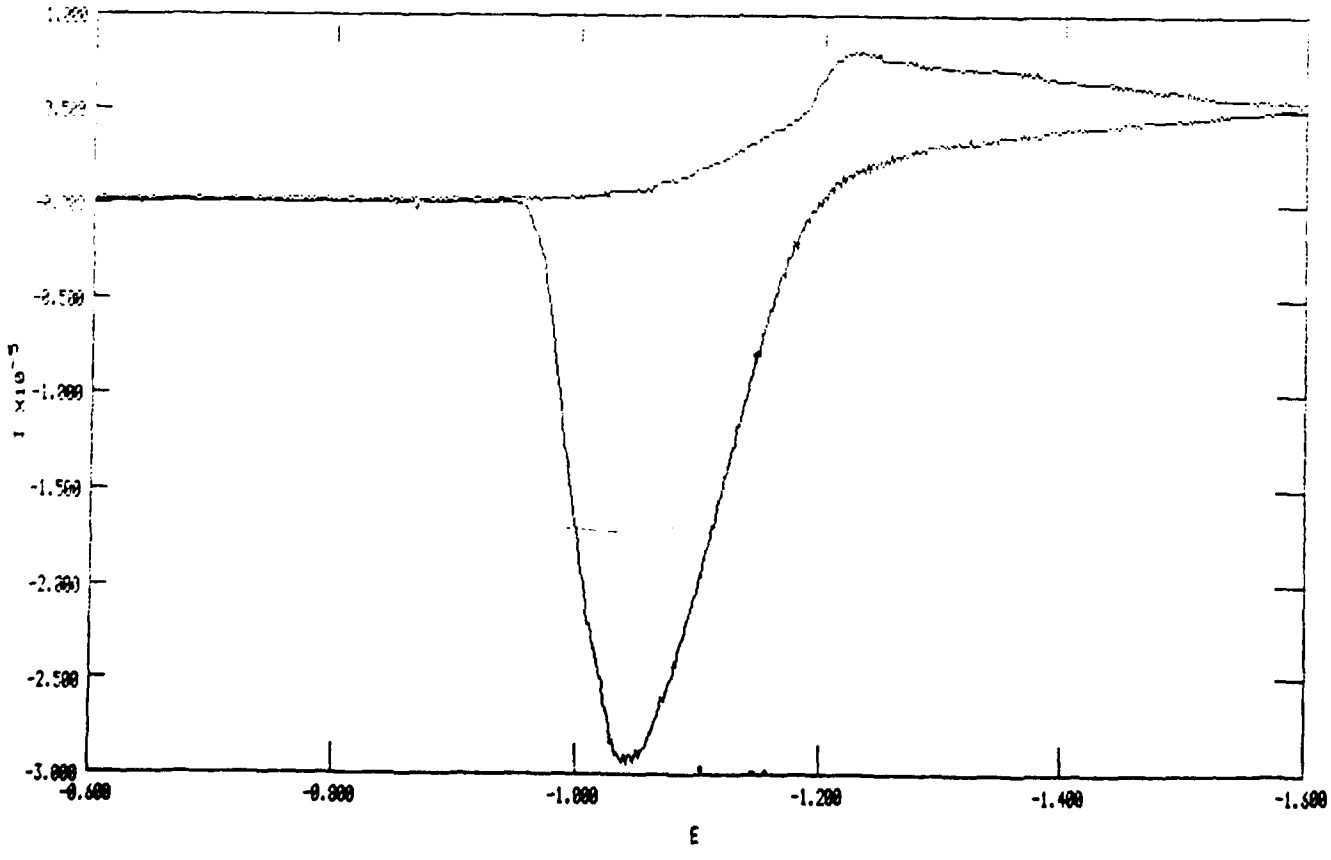

PN Model 270 Electrochemical Analysis Software FV 1.00
EXT CV EXPERT CYCLIC VOLTAMMETRY DA 08-02-90 TR 13:16:57
NORMAL PT PASS CP 0.000 vs. OC CT PASS DT PASS IP -0.400 vs. R ET 2
VI -1.300 vs. R VD PASS V2 0.000 vs. OC FP -0.400 vs. R SI 0.002 SR 5.000E-01 ST 4.000E-03
SC 1 SC 1 AM RAMP CR 100 UA NP 1401 RU 0.000E+00 IR NONE
FL NONE RT HIGH STABILITY
hgnal.dat

Figure 9. Staircase cyclic voltammogram (ν = 500 mV s^{-1}) for deposition and stripping of Na at a mercury film deposited on a 250-μm diameter tungsten electrode. Melt is $AlCl_3$:ImCl (N = 0.53) buffered with NaCl ([Na^+] = 0.56 M).

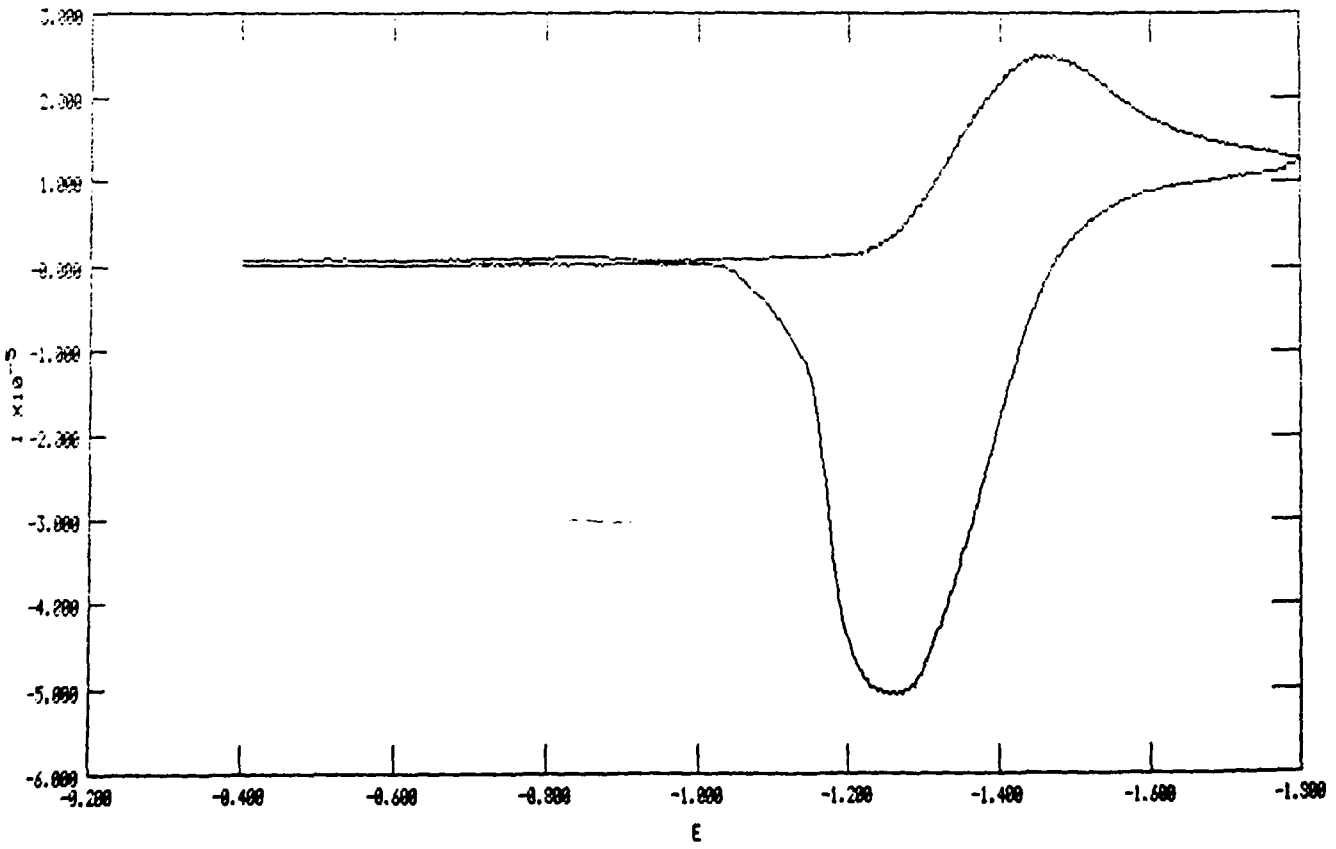

PN Model 270 Electrochemical Analysis Software FV 1.00
EXT CV EXPERT CYCLIC VOLTAMMETRY DR 08-02-90 TR 15:49:04
NORMAL PT PASS CP 0.000 vs. OC CT PASS DT PASS IP -0.400 vs. R ET 2
VI -2.100 vs. R VD PASS V2 0.000 vs. OC FP -0.400 vs. R SI 0.002 SR 2.000E-01 ST 1.000E-02
NC 1 SC 1 AM RAMP CR 100 UA NP 1701 RU 0.000E+00 IR NONE
FL NONE RT HIGH STABILITY
hgk5.dat

Figure 10. Staircase cyclic voltammogram (ν = 200 mV s^{-1}) for deposition and stripping of K at a mercury film deposited on a 250-μm diameter tungsten electrode. Melt is $AlCl_3$:ImCl (N = 0.53) buffered with KCl (K^+] = 0.56 M).

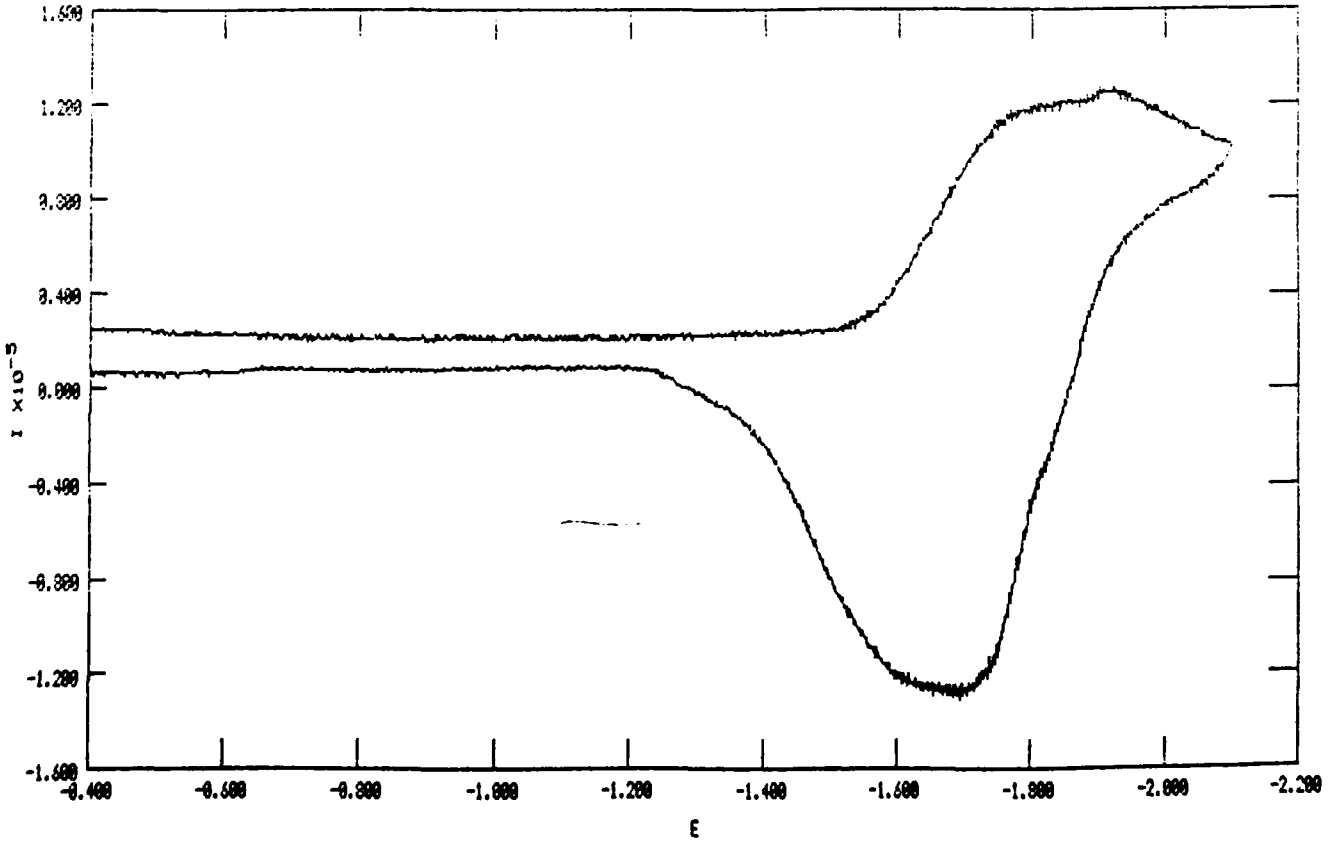

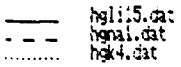

Figure 11. Staircase cyclic voltammograms (ν = 500 mV s^{-1}) for deposition and stripping of (a) Li, (b) Na, and (c) K at a mercury film deposited on a 250-μm diameter tungsten electrode. Melts are $AlCl_3$:ImCl (N = 0.53) buffered with the appropriate alkali metal chloride.

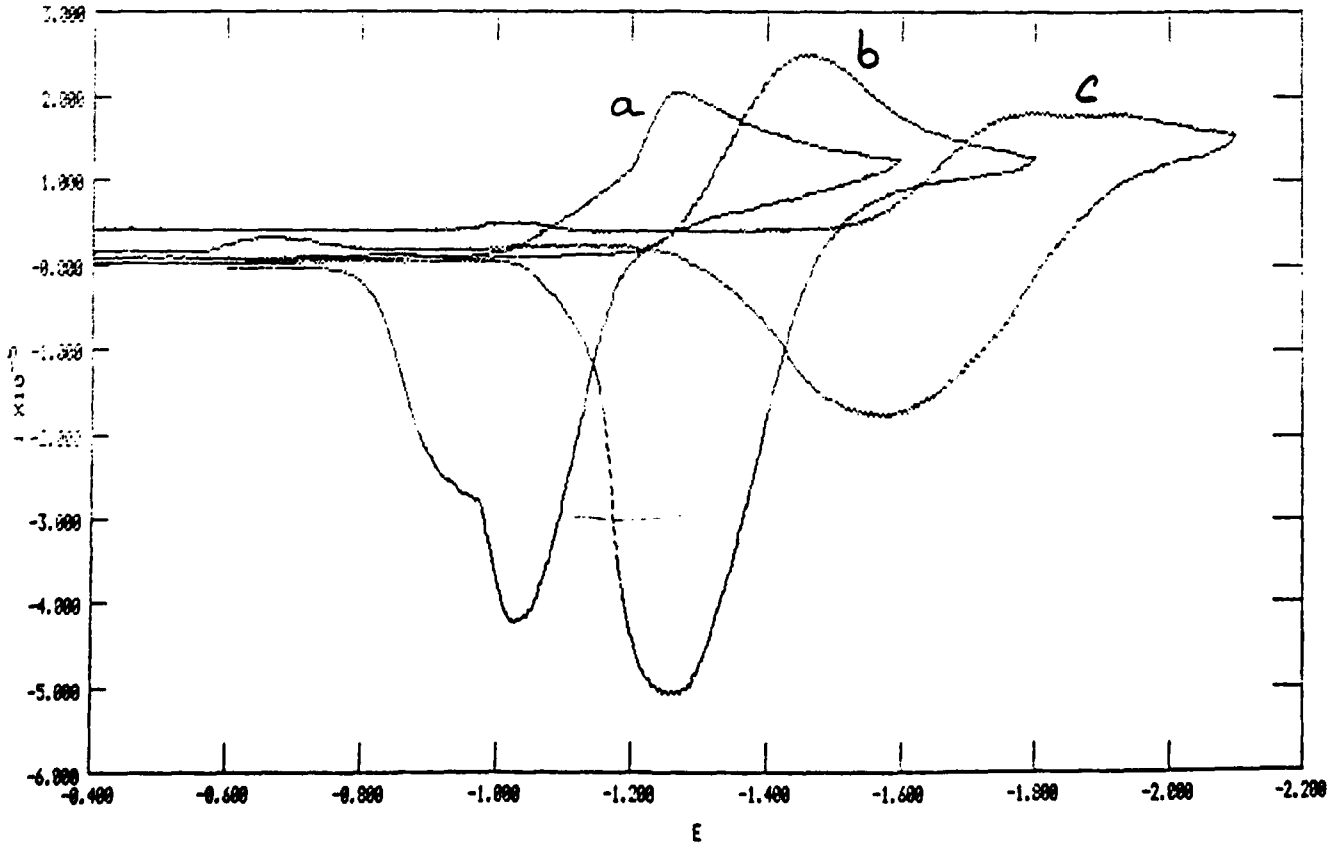

PM Model 270 Electrochemical Analysis Software FV 1.00
EXT CV EXPERT CYCLIC VOLTAMMETRY DA 09-02-90 TM 13:42:29
NORMAL PT PASS CP 0.000 vs. OC CT PASS DT PASS IP -0.409 vs. R ET 2
EI -2.000 vs. R VD PASS V2 0.000 vs. OC FP -0.400 vs. R SI 0.002 SR 2.001E-02 ST 9.997E-02
NC 1 SC 1 AM RAMP CR 10 UA NP 1601 RU 0.000E+00 IR NONE
FL NONE RT HIGH STABILITY
hgna6.dat

Figure 12. Staircase cyclic voltammogram ($\nu = 20$ mV s^{-1}) for deposition and stripping of Na at a mercury film deposited on a 250-μm diameter tungsten electrode. Melt is $AlCl_3$:ImCl (N = 0.53) buffered with NaCl ($[Na^+] = 0.56$ M).